ELSEVIER

Polymer 44 (2003) 123–136

polymer

www.elsevier.com/locate/polymer

Rubber toughened semicrystalline PET: influence of the matrix properties and test temperature

Wendy Loyens, Gabriël Groeninckx*

Department of Chemistry, Laboratory of Macromolecular Structural Chemistry, Katholieke Universiteit Leuven (KULeuven), Celestijnenlaan 200F, B-3001 Heverlee, Belgium

Received 5 June 2002; received in revised form 22 August 2002; accepted 10 October 2002

Abstract

This article is concerned with the effect of the inherent matrix properties (matrix molar mass and crystallinity) as well as the temperature on the impact behaviour of rubber toughened semicrystalline polyethylene terephthalate (PET). The dispersed phase consists of a blend of an ethylene-*co*-propylene rubber (EPR) and a copolymer of ethylene and 8 wt% glycidyl methacrylate (E-GMA8) acting as a compatibilising agent, leading to PET/(EPR/E-GMA8) blends. The influence of the matrix molar mass on the impact behaviour of rubber toughened PET is found to primarily originate from its effect on the blend phase morphology, rather than from an inherent effect of the molar mass itself. The dispersed phase particle size is seen to decrease with increasing PET molar mass. A direct correlation between the impact strength and the interparticle distance could be established. A critical interparticle distance (ID_c) of 0.1 μm could be determined, independent of the PET molar mass. The brittle–ductile transition temperature (T_{bd}) of the blends with a varying matrix molar mass also displayed a strong correlation with the interparticle distance, independent of the matrix molar mass. However, this correlation appears to depend on the crystalline characteristics of the PET matrix material since an incompletely crystallised PET matrix leads to an increase of the T_{bd}.

Keywords: Semicrystalline polyethylene terephthalate; Rubber modification; Matrix properties; Brittle–ductile transition temperature

1. Introduction

The morphological characteristics of thermoplastic polyethylene terephthalate (PET)/rubber blends are extremely important with respect to the improvement of the impact toughness through rubber modification [1]. Reactive compatibilisation is needed to obtain finely dispersed phase morphologies and a stable matrix/rubber interface [1–9]. In literature, attention is most often focussed on the parameters influencing the phase morphology development and the impact response of rubber toughened polymers (e.g. type and content of rubber modifier, type and content of reactive compatibiliser, viscosity ratio and mixing conditions) [8–15]. However, much less attention has been paid to the influence of the inherent matrix characteristics (i.e. molar mass and crystallinity). The main difficulty encountered when investigating the correlation between the matrix properties and the impact behaviour of rubber toughened semicrystalline thermoplastics, is the simultaneous influence of the matrix properties on the blend phase morphology. Varying the matrix molar mass implies a variation of its melt viscosity. Previously, Dijkstra and Gaymans [14] reported on the effect of the nylon6 matrix molar mass by mixing a nylon6/polybutadiene masterbatch with a high or low molar mass nylon6. The matrix molar mass was reported to have a strong effect on the impact behaviour. Paul et al. [16–18] studied the effect of the matrix molar mass on the morphology development and the impact behaviour of rubber toughened nylon6 and polybutylene terephthalate (PBT). The influence of the polypropylene (PP) molar mass has been studied for PP/ethylene-*co*-propylene diene rubber (EPDM) blends [19].

Fundamental research concerning the effect of the matrix crystallinity on the impact behaviour of rubber toughened thermoplastics is rather rare. Van der Wal et al. [19] studied the influence of the PP crystallinity on the blend morphology and the impact response of PP/EPDM blends.

* Corresponding author. Tel.: +32-1632-7440; fax: +32-1632-7990.
E-mail address: gabriel.groeninckx@chem.kuleuven.ac.be (G. Groeninckx).

0032-3861/03/$ - see front matter © 2002 Elsevier Science Ltd. All rights reserved.
PII: S0032-3861(02)00743-7

Table 1
Matrix materials and dispersed phase components

Designation	Product name	Supplier	M_n[a] (g/mol)	Torque value[b] (N m)	Impact strength[c] (kJ/m^2)
L-MW PET	–	DSM	18 500	1.9	1.4 ± 0.2
M-MW PET	CaripakG82	Shell	29 500	7.8	2.5 ± 0.1
H-MW PET	–	DSM	38 400	11.1	1.7 ± 0.2
EPR	Vistalon 805	Exxon	100 000	19.3	–
E-GMA8	Lotader AX 8440	Elf Atochem	–	9.5	–

[a] Number average molar mass (M_n) values obtained from the supplier.
[b] Values taken from Haake rheometry after 10 min of mixing at 280 °C and 50 rpm.
[c] Values measured at room temperature on standard notched Izod bars of semicrystalline PET.

Martuscelli et al. [20] investigated the influence of the matrix crystallinity on the tensile properties of various blend systems.

Besides these structural parameters, the test conditions (i.e. test temperature and speed) also exert a distinct influence on the impact behaviour [15,21,22]. The temperature dependence of the deformation behaviour of thermoplastics is well defined by the brittle–ductile transition temperature (T_{bd}). The brittle–ductile transition is characterised by the Ludwig–Davidenkov–Orowan (LDO) criterion, stating that fracture upon loading will proceed in a ductile manner when the fracture stress exceeds a critical value (i.e. increases above the yield stress) [2,22].

Our previous results clearly revealed that the most effective toughening of semicrystalline PET is provided by finely dispersing a preblend of ethylene-*co*-propylene rubber (EPR) and a copolymer of ethylene and 8 wt% of glycidyl methacrylate (E-GMA8) [1]. The latter acts as a compatibilising agent. Accordingly, the present article is concerned with the impact response of the ternary PET/(EPR/E-GMA8) blend system upon varying the matrix molar mass or the matrix crystallinity. Subsequently, also the influence of the temperature during impact testing will be investigated and discussed. Three different PET matrices will be examined, having a relatively low, medium or high molar mass. The PET matrix crystallinity is altered by varying the compression moulding conditions (moulding time and/or temperature) employed for the sample preparation.

2. Experimental

2.1. Materials

The main characteristics of the PET compounds and the dispersed phase components are given in Table 1. The designation of the matrix materials is based on their relative molar mass. The medium-molar mass (i.e. medium-molecular weight) (M-MW) PET compound is a commercial grade from Shell ($\rho = 1.40$ g/cm^3). Both the low-molar mass (L-MW) and the high-molar mass (H-MW) PET compounds are not commercially available. They were kindly prepared and provided by DSM Research. The EPR rubber has an *E*/*P* ratio of 78/22 ($\rho = 0.86$ g/cm^3) and was kindly supplied by Exxon Chemical. The reactive compatibiliser used is the Lotader AX 8440 grade from Elf Atochem, displaying an elastomeric behaviour (MFI (190 °C, 2.16 kg) = 5 g/10 min).

2.2. Blend preparation and compounding

Before blending with PET, EPR and E-GMA8 were preblended at different ratios in a Haake Rheocord 9000 batch mixer using a small mixing chamber (69 cm^3) at a temperature of 180 °C and a screw speed of 50 rpm during 5 min. Prior to mixing, all materials were dried overnight under vacuum. The compounding of the rubber modified materials was performed on the Haake batch mixer using a mixing chamber of 300 cm^3 at a temperature of 280 °C, a screw speed of 50 rpm and a mixing time of 10 min. The compositions of the ternary PET/(EPR/E-GMA8) blends are based on a constant weight concentration of the dispersed phase but with a changing ratio (EPR/E-GMA8) of the two dispersed phase components [1]. For further analysis, the blends were compression moulded into plaques. After initial melting and pressing at 280 °C, the mould was transferred into a second press held at a temperature of 180 °C for the final moulding step (5 min). The compression moulding procedure was carried out carefully in order to control the crystallisation conditions. The influence of the matrix crystallinity is studied by changing either the temperature or the duration of the final compression step.

2.3. Rheological analysis

During the melt-blending process in the Haake batch mixer, a simultaneous measurement of the torque was performed. This torque value is considered a measure of the viscosity of the mixture present in the mixing chamber.

2.4. Morphological analysis

Scanning electron microscopy (SEM) was performed on small pieces taken from the compression moulded plaques using a Philips XL-20 scanning electron microscope. The

samples were smoothed on a Leica Ultracut UCT microtome at −100 °C and afterwards etched in *m*-xylene at 105 °C to remove the minor phase. Quantitative morphological analysis was performed using Leica Qwin image analysis software.

2.5. Notched Izod impact testing

Notched Izod impact tests were performed according to ISO-180 on a Zwick 5110 apparatus. The samples ($63 \times 10 \times 4$ mm^3) were machine-cut from compression moulded plaques. The notch was milled in, having a depth of 2 mm, an angle of 45° and a notch radius of 0.25 mm. Prior to testing, the samples were dried overnight and subsequently acclimatised for 1 h at the respective test temperature. At each temperature, at least five samples were tested and their results averaged.

2.6. Thermal analysis

The crystallisation behaviour of the blend components is characterised with a Perkin Elmer Pyris-1 DSC on samples from the compression moulded plaques. They were heated from −80 to 290 °C at 10 °C/min. The mass matrix crystallinity is calculated from the experimental heat of fusion measured during the heating run, according to Eq. (1). When matrix cold crystallisation was present, the corresponding crystallisation enthalpy was subtracted from the melt enthalpy

$$X_c = \frac{\Delta H_{m(PET)}}{\Delta H^0_{m(PET,100\%)}} - \frac{|\Delta H_{c(PET)}|}{\Delta H^0_c(T)} w^{-1}_{PET} \times 100\% \quad (1)$$

with X_c = mass crystallinity, $\Delta H^0_{m(PET,100\%)}$ =heat of fusion of 100% crystalline PET (140.1 J/g from the ATHAS databank), $\Delta H_{m(PET)}$ =melt enthalpy of PET, $|\Delta H_{c(PET)}|/\Delta H^0_c(T)$ =(cold) crystallisation enthalpy of PET corrected for the temperature dependence of the crystallisation enthalpy (105.0 J/g) and w_{PET} = PET weight fraction in the blend.

2.7. Wide angle X-ray diffraction

WAXD measurements were performed using a Rigaku Rotaflex RU-200B rotating anode device. Diffraction patterns of compression moulded samples were obtained in the reflection mode from 5 to 60° 2θ.

3. Results and discussion

3.1. Matrix molar mass effect

3.1.1. Influence of the matrix molar mass on the blend rheology

Torque rheometry has proven to be a valid tool for

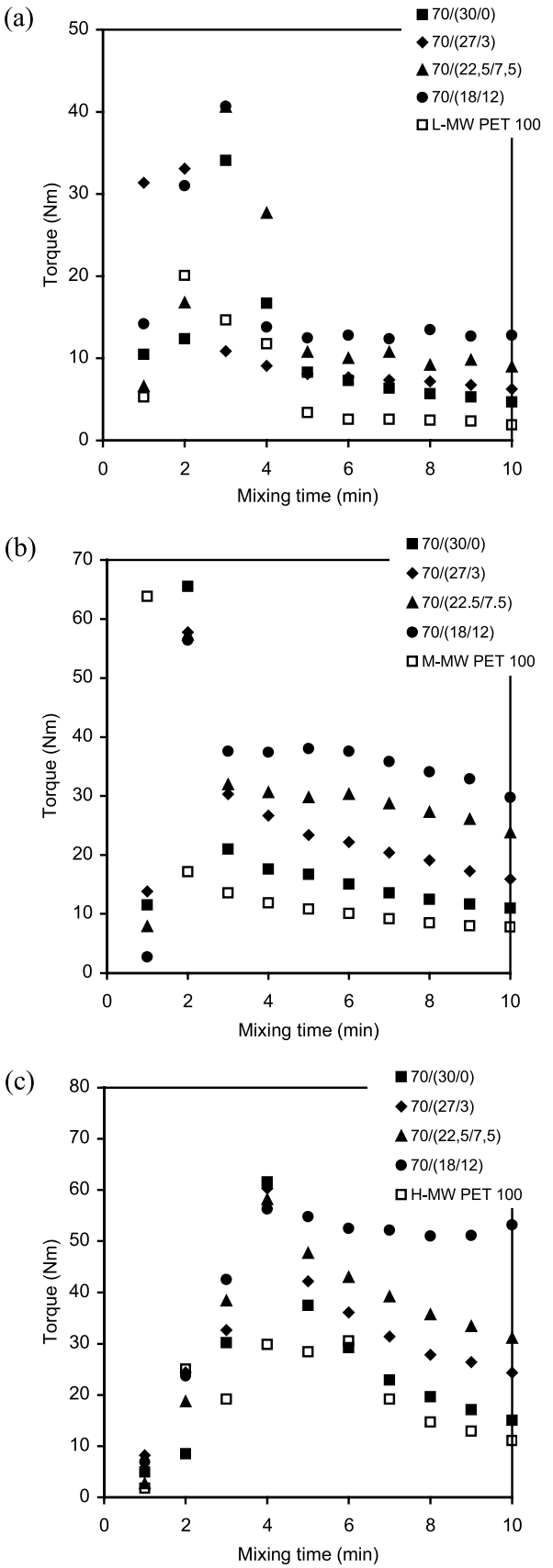

Fig. 1. Torque values as a function of the mixing time for the blends with a dispersed phase concentration of 30 wt% and a varying EPR/E-GMA8 ratio for the following PET matrix molar masses. (a) L-MW, (b) M-MW, and (c) H-MW.

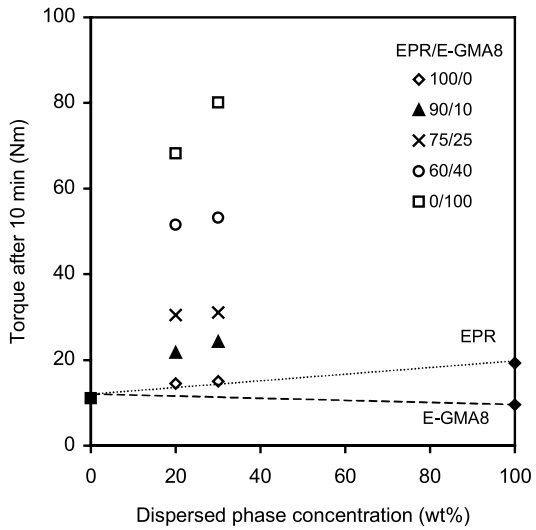

Fig. 2. Torque value after 10 min of mixing for the H-MW PET blends as a function of the dispersed phase concentration with a varying E-GMA8 content.

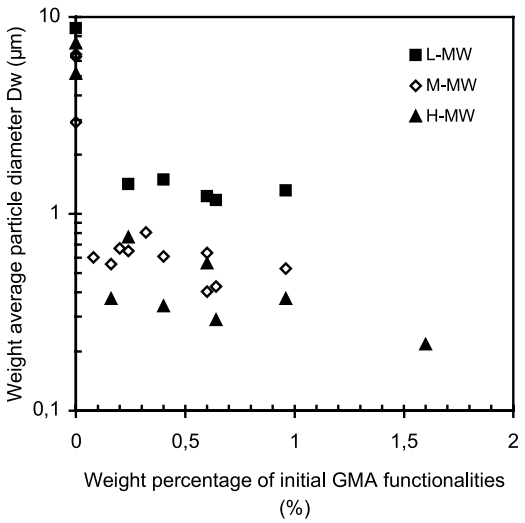

Fig. 4. Weight average particle diameter for the blends with a varying matrix molar mass as a function of the concentration of GMA functionalities present in the blend.

evaluating the rheological response of both the pure materials and their respective reactively compatibilised blends [6,7,23]. Increasing the matrix molar mass (M_n) involves a corresponding increase of the melt viscosity of the material, as can be seen from the increased torque values of the pure PET compounds (Table 1).

Fig. 1 provides an overview of the torque response as a function of the mixing time for the 70/(x/y) blends, having different PET matrix molar masses. Although the matrices differ, the course of the torque response is seen to be fairly similar. After the initial feeding period, the torque tends to rise slightly, indicative of the occurrence of a chemical reaction. Thereafter, the torque decreases and levels off to reach a plateau value. Increasing the E-GMA8 content in the dispersed phase is seen to lead to increasingly higher melt viscosities. This becomes more clear from Fig. 2 presenting

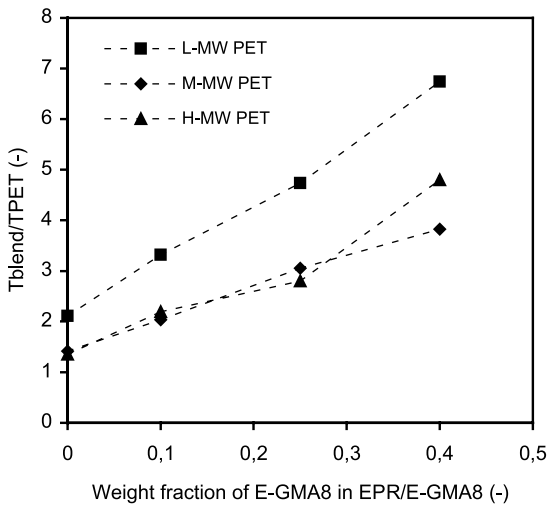

Fig. 3. Relative torque value (T_{blend}/T_{PET}) after 10 min for the 70/(x/y) blends as a function of the weight fraction of E-GMA8 in the dispersed phase.

the torque values after 10 min of mixing as a function of the dispersed phase concentration for the H-MW blends. The reactively compatibilised blends display high torque values, located well above the non-reactive additivity line. This non-reactive baseline is constructed from the composition-weighted average of the torque values of the individual components. The increased values distinctly illustrate the occurrence of the compatibilisation reaction between GMA and the PET end groups. This has been reported and extensively discussed previously [23].

From Fig. 1, it might be concluded that the torque value of the blends with an equal composition but a different PET matrix molar mass, increases as the matrix molar mass increases. However, when considering the relative torque ratios (T_{blend}/T_{PET}), it follows that both the M-MW and the H-MW PET blends display comparable values (Fig. 3). This implies that the observed torque increase is primarily related to the increased viscosity of the respective PET matrix. The L-MW PET blends display higher torque ratios, indicating that besides the compatibilisation reaction, possible side reactions have taken place. Increasing the compatibiliser content is observed to increase the overall blend viscosity.

3.1.2. Influence of the matrix molar mass on the blend morphology

The morphology development of a polymer blend during processing is known to be controlled by the competition between droplet break-up and coalescence [3,24,25]. The final particle size depends on the viscosity of the respective blend components, the viscosity ratio, the interfacial tension and the applied shear rate. Since an increase of the matrix molar mass is accompanied by an increase of the matrix viscosity, this is expected to affect the morphology. Fig. 4 presents the particle diameter for blends with a varying PET matrix molar mass as a function of the concentration of the

Table 2
Weight average particle diameter D_w (μm) as a function of the dispersed phase concentration and composition for three different PET matrix molar masses

Weight fraction of E-GMA8 in dispersed phase	Weight average particle diameter D_w (μm)		
	L-MW PET	M-MW PET	H-MW PET
20 wt%			
0	–	6.45 ± 0.61	5.16 ± 1.50
0.1	–	0.55 ± 0.08	0.37 ± 0.02
0.25	1.49 ± 0.09	0.61 ± 0.09	0.34 ± 0.03
0.4	1.17 ± 0.22	0.43 ± 0.08	0.29 ± 0.03
30 wt%			
0	8.77 ± 1.00	9.49 ± 0.91	7.37 ± 1.20
0.1	1.42 ± 0.06	0.65 ± 0.09	0.76 ± 0.11
0.25	1.23 ± 0.13	0.41 ± 0.03	0.56 ± 0.04
0.4	1.31 ± 0.14	0.53 ± 0.04	0.55 ± 0.11

GMA functionalities present. As expected, the non-compatibilised PET/EPR blends display a coarse morphology, irrespective of the matrix molar mass. The addition of the E-GMA8 compatibiliser is seen to induce a strong decrease of the dispersed phase particle size.

From Fig. 4 and Table 2 it follows that further increasing the GMA concentration (i.e. E-GMA8 content in the EPR/E-GMA8 phase at a constant dispersed phase concentration) does not lead to a further decrease of the particle size for the L-MW and M-MW PET blends. Hence, a low E-GMA8 content is sufficient to obtain a finely dispersed phase morphology. The particle size is nearly independent of the dispersed phase concentration. This effect is often observed when a good interfacial interaction is obtained [26]. The particle size of the H-MW blends displays a stronger dependence on the dispersed phase concentration and composition. This is believed to originate from a decreased end group concentration upon increasing the matrix molar mass, resulting in a lower degree of interfacial grafting. The blend phase morphologies of the different blend systems are illustrated by the SEM micrographs in Fig. 5.

Table 2 reveals that the particle size decreases with increasing PET matrix molar mass. This trend is less pronounced for higher dispersed phase concentrations. The particle size initially decreases strongly with M_n, but tends to reach a plateau value at high M_n levels for the 30 wt% blends (Fig. 6). This levelling off has also been reported by Oshinski et al. [12] for nylon6/styrene–ethylene/butylene–styrene grafted maleic anhydride (SEBS-*g*-MA) blends. The matrix molar mass is thus clearly found to have a strong influence on the final phase morphology of rubber modified PET. Other authors have reported similar correlations between the particle diameter and M_n for various blend

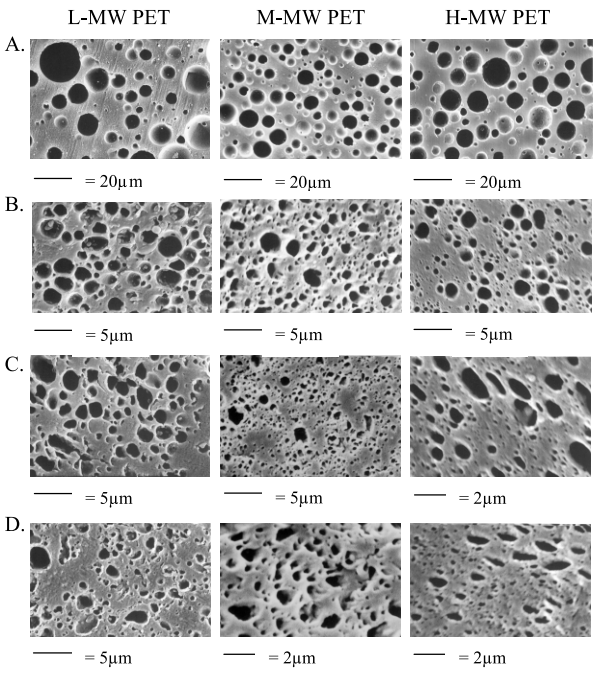

Fig. 5. SEM micrographs illustrating the blend phase morphologies of the different PET matrix molar mass blends. The blend composition varies as follows: (A) 70/(30/0), (B) 70/(27/3), (C) 70/(22.5/7.5), and (D) 70/(18/12).

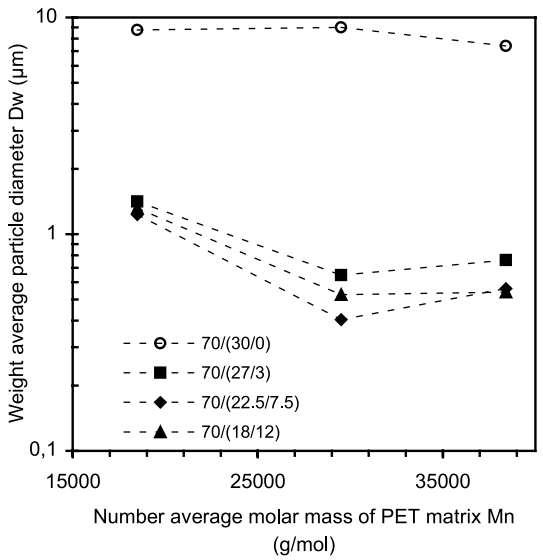

Fig. 6. Weight average particle diameter of the 30 wt% rubber blends as a function of the PET matrix molar mass for various EPR/E-GMA8 ratios.

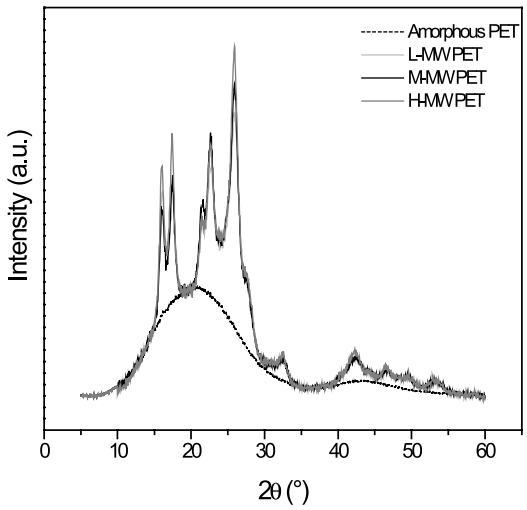

Fig. 7. WAXD diffraction spectra of amorphous PET and semicrystalline PET having a varying matrix molar mass.

systems [12,18,19,27]. The influence of the molar mass originates from several mechanisms [12,27]. As the matrix molar mass increases, the corresponding increase of the melt viscosity leads to an increase of the dispersive shear forces which facilitates the droplet break-up process. A second effect of the increased molar mass consists of a decrease of the viscosity ratio (dispersed phase/PET), which generally leads to a refinement of the morphology [3]. A decreased rate of coalescence with increasing matrix molar mass provides an additional factor for particle size reduction [24].

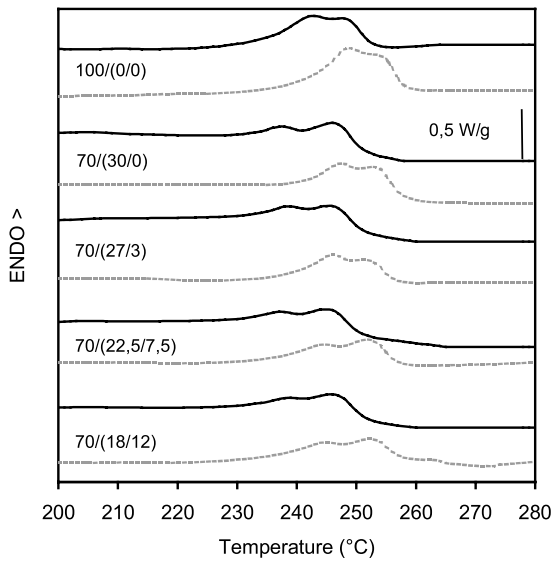

Fig. 8. DSC first heating endotherms of the 30 wt% rubber blends having a medium (—) and a high (- - -) PET matrix molar mass.

Besides the GMA induced compatibilisation reaction, the occurrence of possible side reactions needs to be considered. It can be seen from Fig. 5 that both the L-MW and M-MW PET blends, having a high E-GMA8 content, no longer display completely spherical particles. This phenomenon is less pronounced for the H-MW PET blends. Torque rheometry already revealed increased torque values at high E-GMA8 contents, although the particle size did not change significantly (Fig. 3 and Table 2). In our previous publication [23] and in the literature [28,29], this phenomenon has been attributed to the occurrence of crosslinking reactions. Crosslinking can take place on account of the difunctionality of the PET matrix and/or the formation of secondary hydroxyl groups upon reactive compatibilisation. When the PET molar mass is reduced, the number of reactive end groups is higher, increasing the extent of the crosslinking reactions. Hence, the phenomenon becomes more pronounced for a lower PET molar mass, explaining the high torque ratios observed for L-MW PET blends (Fig. 3). For a high PET molar mass, the number of reactive end groups is lower and will preferentially react according to the interfacial compatibilisation reaction.

The influence of the PET molar mass on the matrix crystallinity was verified from WAXD and DSC experiments. Only a minor increase of the crystallinity from 41.5 to 44.5% could be detected by WAXD when going from L-MW to H-MW PET. The diffraction spectra depicted in Fig. 7 clearly display a strong resemblance, independent of the PET molar mass. This agrees well with literature where it was reported that the molar mass does not have a strong influence on the crystallinity, especially for higher molar masses [30]. Fig. 8 provides an overview of the DSC first heating endotherms of the M-MW and H-MW PET 70/(x/y) blends. As the DSC samples were taken from the Izod impact bars, the first heating results represent the crystalline characteristics as present after compression moulding. The H-MW PET blends display higher melt temperatures compared to the M-MW PET blends, indicating slightly

Table 3
PET mass crystallinity for the 30 wt% rubber modified blends as a funtion of the dispersed phase composition and PET molar mass

Weight fraction of E-GMA8 in dispersed phase	Mass crystallinity of PET matrix (%)	
	M-MW PET	H-MW PET
0	31.2	25.9
0.1	34.1	22.4
0.25	31.7	24.5
0.4	31.4	24.3
Pure PET	23.5	25.7

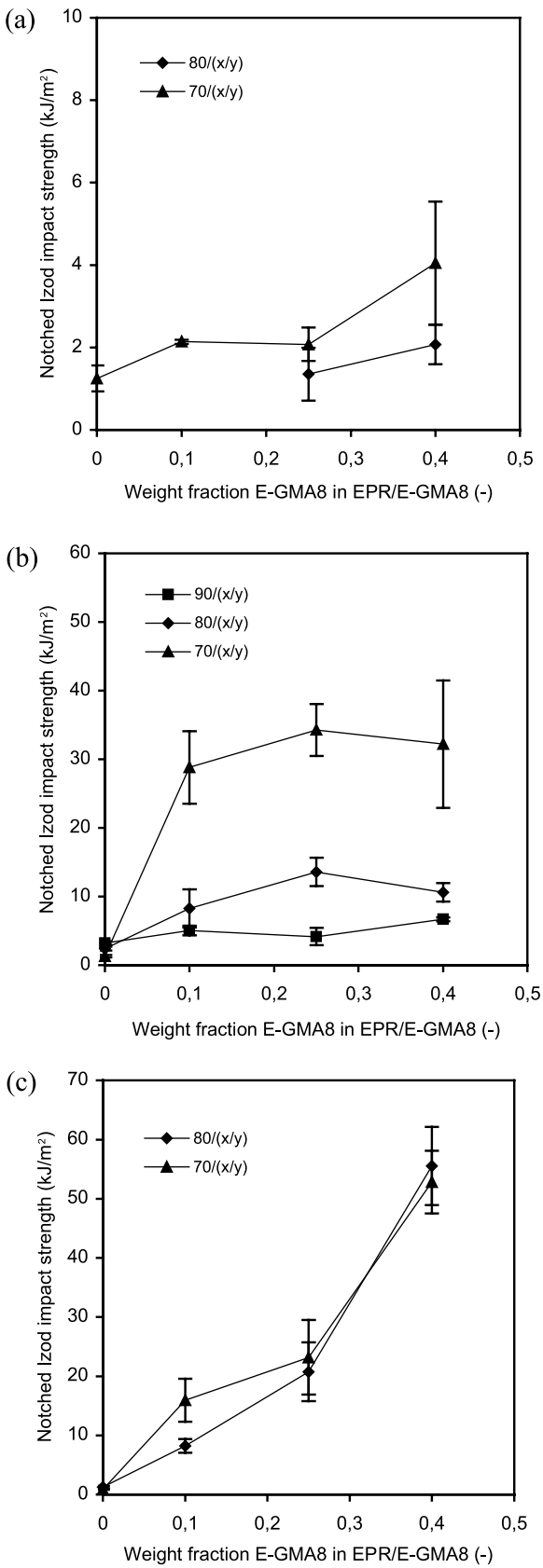

Fig. 9. Notched Izod impact strength at room temperature as a function of the weight fraction of E-GMA8 in EPR/E-GMA8 for various dispersed phase concentrations, and the following PET matrix molar mass. (a) L-MW, (b) M-MW, and (c) H-MW.

higher lamellar thicknesses of the H-MW PET spherulites. Regardless of the matrix molar mass, the blends display double melting endotherms typical for PET. The PET mass crystallinities are derived from the heat of fusion of the first heating run (Eq. (1)) and are presented in Table 3. Pure H-MW PET displays a slightly higher crystallinity, in good agreement with the WAXD observations. The crystallinities of rubber toughened H-MW PET are situated in the vicinity of the crystallinity of pure H-MW PET. In contrast, the rubber toughened M-MW PET compounds have distinctly higher crystallinities when compared to pure M-MW PET. This phenomenon has been discussed in our previous publication [1]. A nucleating activity of the dispersed phase can be held responsible, although this could not be established unambiguously. The reason for the apparent difference when varying the PET molar mass remains unclear.

3.1.3. Influence of the matrix molar mass on the impact behaviour at room temperature

The notch sensitivity of semicrystalline PET becomes quite apparent from the very low notched Izod impact strengths presented in Table 1. It has already been demonstrated that the impact behaviour of PET can be strongly improved by rubber modification [1]. Fig. 9(a)–(c) illustrates the notched Izod impact strength at room temperature for rubber modified PET compounds with a varying PET molar mass. The impact behaviour is found to be highly dependent on the matrix molar mass. The L-MW PET blends display very low impact strengths (<5 kJ/m^2) and a brittle fracture mode characterised by a high fracture speed, a complete separation of the sample halves and the absence of stress whitening. Despite the dispersion of rubber particles, the growing crack is insufficiently stabilised. The impact behaviour of the M-MW PET blends has been described in detail in our previous publication [1]. The 10 and 20 wt% rubber modified blends fail in a brittle manner with relatively low impact strengths (Fig. 9(b)). In contrast, the 30 wt% rubber blends display a clearly ductile fracture mode with a high amount of stress whitening. The sample halves remain attached by a very small ligament at the end of the fracture zone, typical of a ductile fracture [31]. The addition of a low amount of E-GMA8 is sufficient to induce a strong improvement of the impact strength. The impact strength levels off for a further increase of the E-GMA8 content.

The majority of the H-MW PET blends fail according to a ductile fracture mode. The impact strength is highly dependent on the dispersed phase composition. The addition of a small amount of E-GMA8 does not induce a steep increase of the impact strength. Further increasing the E-GMA8 content increases the impact strength, independent of the dispersed phase concentration, resulting in a marked toughness improvement at high E-GMA8 contents.

It can now be concluded that the matrix molar mass is a

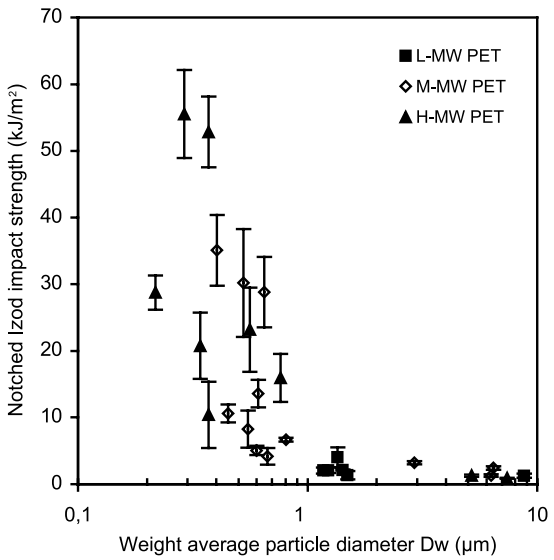

Fig. 10. Notched Izod impact strength as a function of the weight average particle diameter for the investigated PET/(EPR/E-GMA8) blends with varying PET matrix molar mass.

very influential parameter on the impact strength of rubber modified PET. A minimum molar mass is needed to obtain tough materials at room temperature. In order to establish the specific correlation between the matrix molar mass and the impact response, it is essential to take into account the effect of the matrix molar mass on the structural blend characteristics. Although a difference in the PET crystallinity between the M-MW and H-MW PET blends was found, no direct correlation with respect to the impact behaviour could be established. Fig. 10 presents the notched Izod impact strength as a function of the weight average particle diameter for the different blends. A decrease of the particle size is seen to lead to an increase of the impact strength and a transition of the fracture mode. Although several compositions have particle sizes within the 'ductile range', they still display a low impact strength and a brittle fracture mode. The correlation between the impact properties and the particle size is thus not unambiguous. The dispersed phase concentration is also found to be an important factor. Both morphological features can be combined into the interparticle distance parameter, as described by Eq. (2)

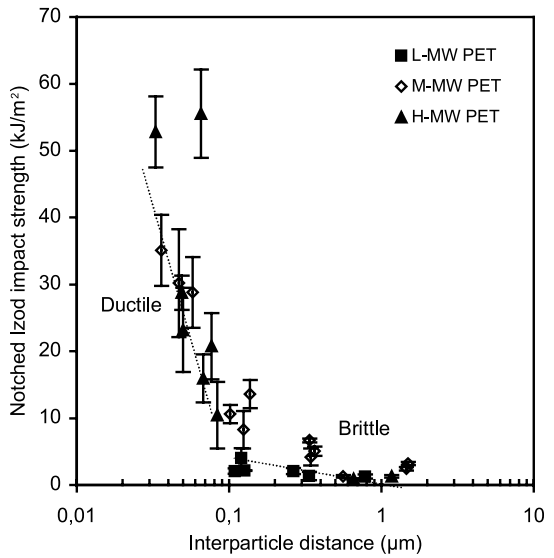

Fig. 11. Notched Izod impact strength as a function of the interparticle distance for the investigated PET/(EPR/E-GMA8) blends with varying PET matrix molar mass.

$$\mathrm{ID} = D\left[\left(\frac{\pi}{6\phi_r}\right)^{1/3} - 1\right] \tag{2}$$

where D is the dispersed phase particle diameter; ID, the interparticle distance; ϕ_r is the rubber volume concentration [3]. The interparticle distance is defined as the matrix ligament thickness between two adjacent rubber particles and needs to be lower than a critical value (ID_c) in order to induce a ductile fracture mode. The respective interparticle distances can be calculated from the quantitative morphological data and are presented in Fig. 11.

There clearly exists a strong correlation between the impact strength and the interparticle distance. The ID_c of the rubber toughened PET compounds can be determined experimentally at approximately 0.1 μm. The ID_c is found to be equal for all blend systems, independent of the PET matrix molar mass. The inability of the L-MW PET blends to display a high impact toughness and ductile fracture mode can now be assigned to their interparticle distances being higher then the ID_c. This is a direct consequence of the influence of the PET molar mass on the dispersed phase morphology. In contrast, the M-MW and H-MW PET compounds display a clear transition of the fracture mode for interparticle distances below 0.1 μm. This brittle–ductile transition is independent of the dispersed phase concentration, as can be seen for the H-MW PET blends. Below ID_c, the impact strength increases linearly with decreasing interparticle distance, which agrees well with earlier observations [3]. The dispersed phase concentration has no influence below ID_c.

It may be concluded that the influence of the PET matrix molar mass on the impact behaviour of rubber toughened PET originates from its direct effect on the phase morphology development, rather than from an intrinsic effect of the molar mass itself. The impact strengths below ID_c can be fitted by a single line, independent of the PET matrix molar mass (Fig. 11).

3.1.4. Influence of the matrix molar mass on the impact behaviour at various temperatures

The brittle–ductile transition temperature is very sensitive to changes of the material parameters and the test conditions [2,22]. A shift of the T_{bd} results from a change in the ratio between the fracture stress and the yield stress. An increase of the matrix molar mass is reported to increase the

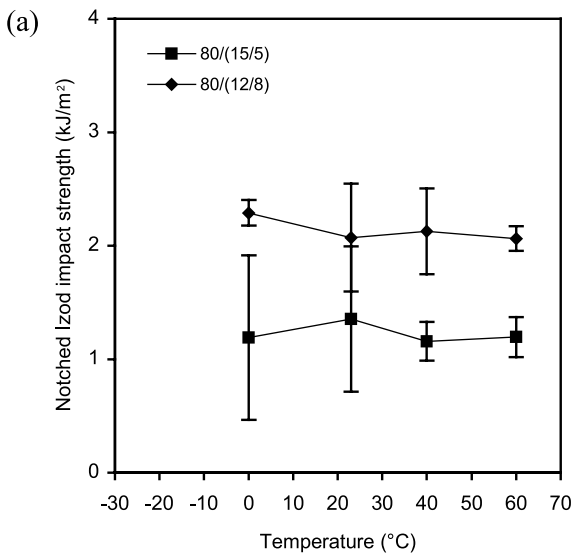

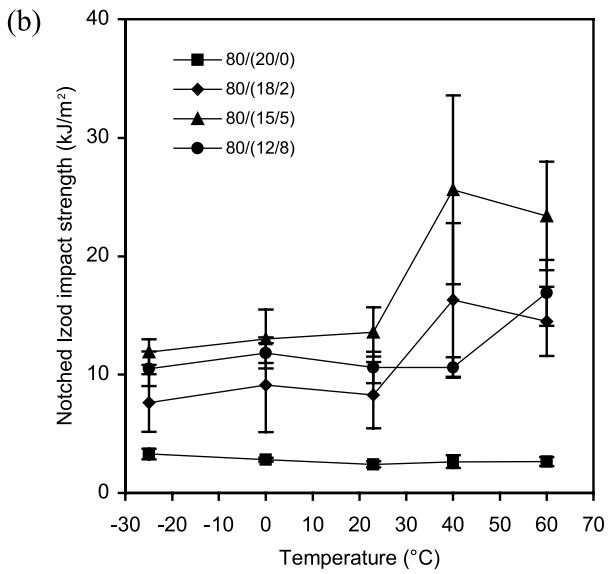

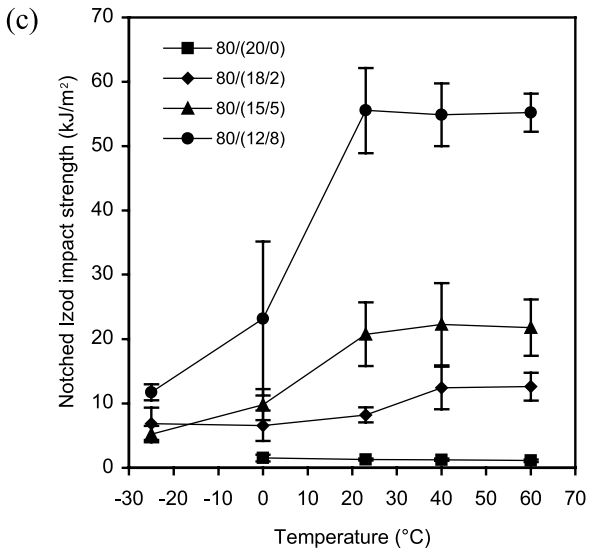

Fig. 12. Notched Izod impact strength as a function of the temperature for the 80/(*x*/*y*) blends having a varying EPR/E-GMA8 ratio and the following PET matrix molar masses. (a) L-MW, (b) M-MW, and (c) H-MW.

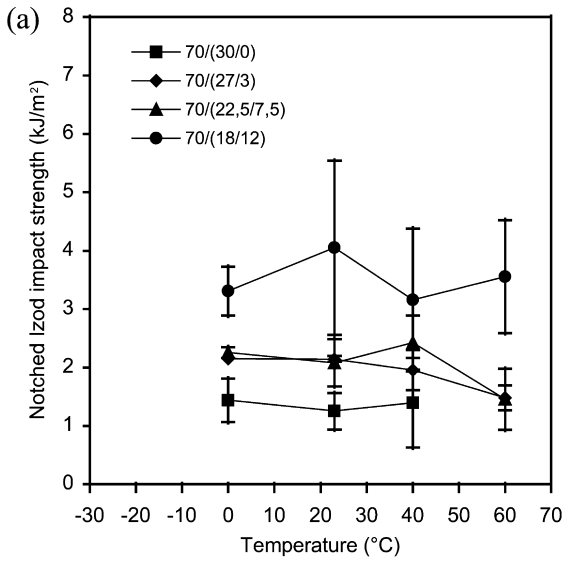

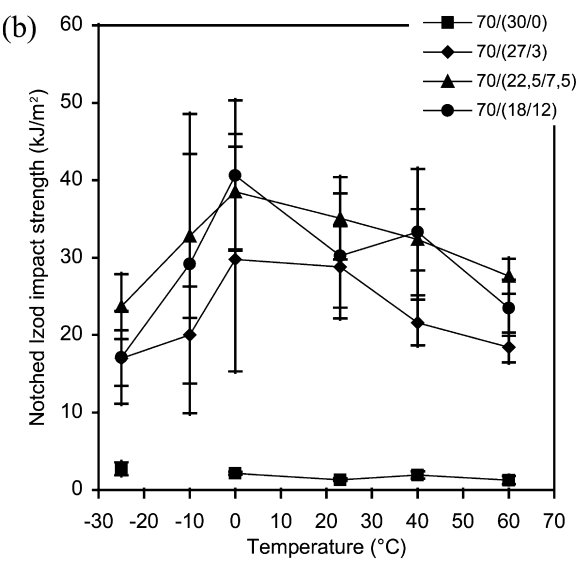

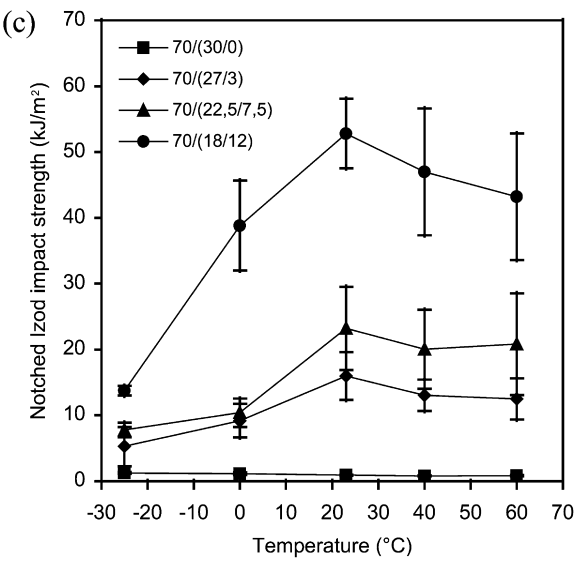

Fig. 13. Notched Izod impact strength as a function of the temperature for the 70/(*x*/*y*) blends having a varying EPR/E-GMA8 ratio and the following PET matrix molar masses. (a) L-MW, (b) M-MW, and (c) H-MW.

Table 4
Brittle–ductile transition temperature of ternary PET/(EPR/E-GMA8) blends as a function of the dispersed phase composition and concentrations for a varying PET matrix molar mass

Weight fraction of E-GMA8 in dispersed phase	Brittle–ductile transition temperature T_{bd} (°C)					
	L-MW PET		M-MW PET		H-MW PET	
	80/(*x*/*y*)	70/(*x*/*y*)	80/(*x*/*y*)	70/(*x*/*y*)	80/(*x*/*y*)	70/(*x*/*y*)
0.1	80	80	40	−5	31	12
0.25	80	80	31	−15	10	8
0.40	80	80	50	−10	7	−12

fracture stress, whereas the yield stress remains unaffected [14,18,19].

Figs. 12 and 13 present the impact strength as a function of the temperature for the blends with a varying PET molar mass, having a total dispersed phase concentration of 20 and 30 wt%, respectively. The brittle–ductile transition temperatures are given in Table 4. The L-MW PET blends display a brittle fracture at all tested temperatures, independent of the concentration and the composition of the dispersed phase. Their actual T_{bd} can be assumed to be situated near the T_g (80 °C) of the PET matrix. The M-MW PET blends with a low dispersed phase concentration (10 wt%) also display a brittle fracture behaviour in the investigated temperature range. Increasing the dispersed phase concentration induces a strong decrease of the T_{bd} (Table 4). The majority of the H-MW blends has a T_{bd} between 0 and 23 °C. The highly ductile 70/(18/12) composition displays a lower T_{bd}, around −12 °C.

These notched impact results reveal some very interesting trends and the influence of the matrix molar mass is not straightforward. For a dispersed phase concentration of 20 wt%, the T_{bd} decreases with increasing matrix molar mass. This correlation has been reported before by a number of authors [14,17–19]. The blends with a dispersed phase concentration of 30 wt% reveal a slightly different trend. The T_{bd} initially decreases with increasing molar mass, but subsequently levels off or even increases for a further increase of the matrix molar mass. In order to establish if there exists a direct correlation between the T_{bd} and M_n, the influence of the matrix molar mass on other blend characteristics (i.e. PET crystallinity and blend phase morphology) needs to be taken into account. The difference in matrix crystallinity when varying the M_n has no direct influence on the T_{bd}, as no unambiguous correlation could be established. As seen before, the matrix molar mass has a strong influence on the morphological characteristics. Fig. 14 presents the T_{bd} as a function of the dispersed phase particle diameter for the M-MW and H-MW PET blends. The T_{bd} is found to decrease with decreasing particle size, which has been reported in literature [17,18]. However, no clear correlation could be established regarding the influence of the matrix molar mass or the dispersed phase concentration. Fig. 15 presents the T_{bd} as a function of the interparticle distance. It becomes apparent that there exists a strong correlation between both characteristics. A decrease of the interparticle distance is accompanied by a decrease of the T_{bd}. It can be concluded that the brittle–ductile transition of the fracture mode is directly related to the

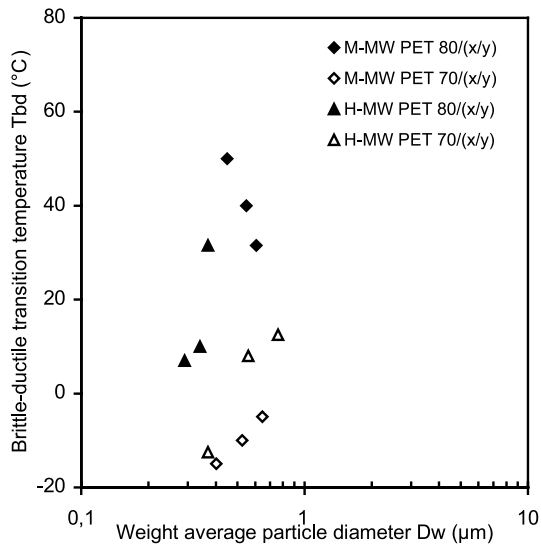

Fig. 14. Brittle–ductile transition temperature as a function of the weight average particle diameter for the M-MW and H-MW PET blends.

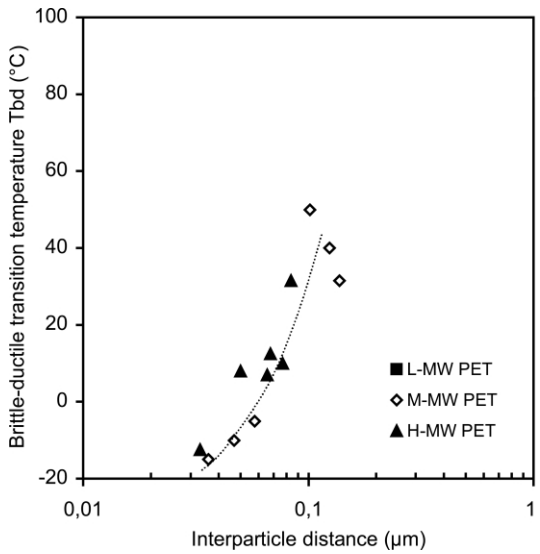

Fig. 15. Brittle–ductile transition temperature as a function of the interparticle distance for the M-MW and H-MW PET blends.

Table 5
Moulding conditions during the final isothermal compression moulding step and the respective crystallinities for pure M-MW PET

Temperature (°C)	Time (min)	X_c[a] (%)
180	0.5	36.9
180	5	42.9
150	5	44.4
23	5	3.5

[a] As determined from WAXD.

interparticle distance. This agrees well with the results reported by Wu and Borggreve et al. [3,5].

Looking closer at the influence of the matrix molar mass, it follows that the T_{bd}s of the different blends tend to follow the same trend. Moreover, the transition temperatures can be fitted reasonably well onto the same curve as a function of the interparticle distance (line drawn to highlight the trend). The influence of the PET molar mass on the T_{bd} thus originates primarily from its effect on the blend phase morphology rather than from an intrinsic effect of the matrix itself. Also for acrylonitrile–butadiene–styrene (ABS) toughened PBT [18], the main effect of M_n on the impact response is reported to originate from its influence on the blend morphology. For rubber toughened nylon6, it was observed that at a constant particle size, the influence of M_n is minimalised at higher values of the molar mass [17].

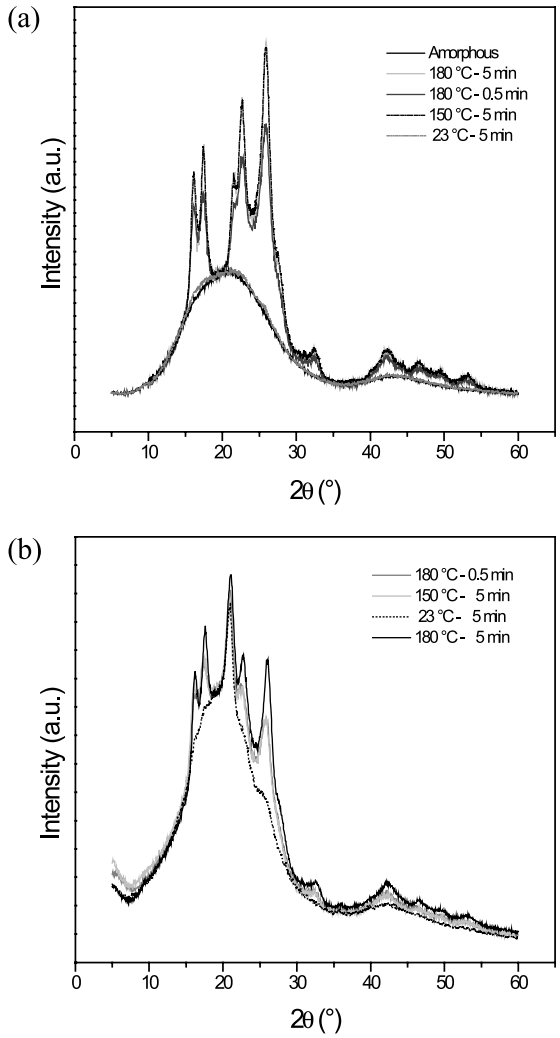

Fig. 16. WAXD diffraction spectra of (a) pure PET and (b) PET/(EPR/E-GMA8) 70/(22.5/7.5) blends prepared at the different isothermal compression moulding conditions.

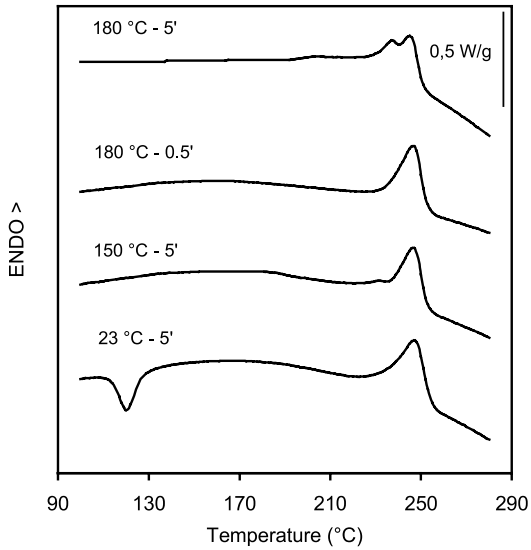

Fig. 17. DSC first heating endotherms of the PET/(EPR/E-GMA8) 70/(22.5/7.5) blend, prepared at different isothermal compression moulding conditions.

3.2. Matrix crystallinity effect

3.2.1. Influence of the matrix crystallinity on the blend morphology

The crystallisation of polymers and more particularly PET is known to be very sensitive to the crystallisation conditions applied (temperature and time) [30,32]. Varying the temperature and/or the duration of the final isothermal compression moulding step will alter the matrix crystallinity.

Table 5 provides an overview of the various crystallisation conditions applied as well as the respective crystallinities of pure PET as determined by WAXD. The PET employed is the medium molar mass compound (M-MW PET). Fig. 16(a) and (b) presents the WAXD diffraction spectra of pure PET and PET/(EPR/E-GMA8) 70/(22.5/7.5) blends, prepared according to the various conditions. The determination of the PET crystallinity in the ternary blends is difficult to perform based on the WAXD spectra, since E-GMA8 also displays several crystalline reflections (21.15 and 23.5°). Accordingly, this PET matrix crystallinity is obtained from the heat of fusion from the first heating DSC endotherms (Fig. 17).

The PET crystallinities are presented in Table 6. It follows that both pure PET and the ternary blends respond fairly similar to the changed moulding conditions. The

Table 6
Characteristic values for pure PET and the PET/(EPR/E-GMA8) 70/(22.5/7.5) blend prepared at the different isothermal compression moulding conditions

Material	ΔH_m (J/g PET)	X_c (%)	D_w (μm)	D_w/D_n	T_{bd} (°C)
Pure PET 180 °C-5′	33	23.5	–	–	–
Blend 70/(22.5/7.5)					
180 °C-0.5′	39.2	28.0	0.40	1.47	7
180 °C-5′	44.4	31.7	0.41	1.47	−15
150 °C-5′	43.5	31.1	0.54	1.49	−5
23 °C-5′	34.5	20.8	0.70	1.44	12

temperature and moulding time can have a dual effect on the matrix crystallisation behaviour. They can affect the primary nucleation process and/or the spherulite growth rate, consequently influencing the overall rate of crystallisation.

PET is well known to display its fastest crystallisation kinetics around 180 °C [30]. It is therefore not surprising that the blend crystallised at 180 °C during 5 min displays a high matrix crystallinity (31.7%). A decrease of the moulding time to 0.5 min leads to a decrease of the matrix crystallinity resulting from an incomplete crystallisation due to the very short residence time. A decrease of the isothermal crystallisation temperature below 180 °C is accompanied by a decrease of the spherulite growth rate [30]. On the other hand, the higher degree of undercooling will also result in the formation of a higher amount of critical nuclei [30,32,33]. The DSC and WAXD results reveal that an isothermal crystallisation temperature of 150 °C during 5 min leads to a matrix crystallinity comparable to that obtained at 180 °C during 5 min. The crystallisation is completely altered when the final moulding step is performed at room temperature (Fig. 16). The PET crystallisation only takes place during cooling until ± 80 °C (T_g of PET). Both the low moulding temperature and moulding time do not permit a fast and complete crystallisation, which results in a decreased matrix crystallinity [33,34]. A significant amount of cold crystallisation can be observed (Fig. 17).

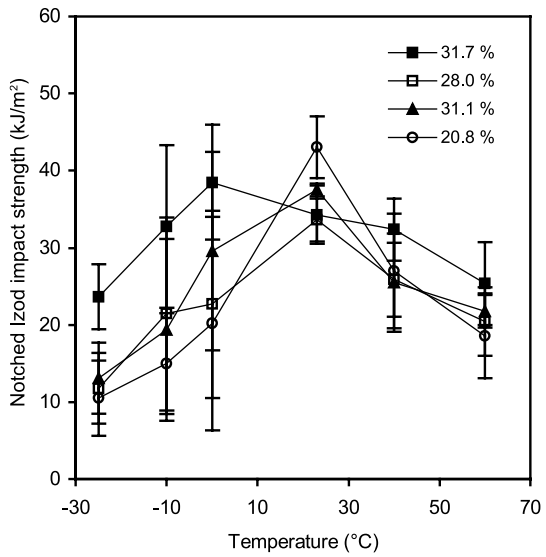

Fig. 18. Notched Izod impact strength of the PET/(EPR/E-GMA8) 70/(22.5/7.5) blend as a function of the temperature and the matrix crystallinity.

In addition, the influence of the changed moulding conditions on the blend phase morphology needs to be considered. The particle diameters and the dispersities (D_w/D_n) of the blends are given in Table 6. It follows that a decrease of the isothermal crystallisation temperature below 180 °C is accompanied by an increase of the particle size. A reduction of the moulding time at constant crystallisation temperature (180 °C) does not affect the blend phase morphology. As the blend is very effectively compatibilised [23] and a decrease of the crystallisation temperature results in an increase of the blend viscosity, it is not likely that the moulding conditions can be held responsible for the observed phase coarsening. In literature, reports on the influence of matrix crystallisation on the blend phase morphology are rare. Martuscelli [33] reported that depending upon the spherulite growth rate, the blend phase morphology of PP/EPDM and PP/EPR blends was influenced. Coalescence of droplets has been reported to occur at high concentrations of the dispersed phase [33,35]. However, it needs to be remarked that the spherulite size of semicrystalline PP is quite high (>100 μm) [36]. The PET spherulites have much smaller dimensions (<1 μm), making it less plausible that the observed difference in particle size is provoked by coalescence induced by the growing spherulite front.

3.2.2. Influence of the matrix crystallinity on the impact behaviour

Fig. 18 presents the impact strengths of the semicrystalline PET/(EPR/E-GMA8) 70/(22.5/7.5) blends as a function of the temperature. The corresponding brittle–ductile transition temperatures are listed in Table 6. The T_{bd} can be seen to decrease with increasing PET matrix crystallinity. It would now seem obvious to claim a direct effect on the impact behaviour. However, the influence of the moulding conditions on the dispersed phase morphology needs to be taken into account. Fig. 19 accordingly presents the T_{bd} as a function of the interparticle distance. The T_{bd} is seen to decrease with decreasing interparticle distance, irrespective of the matrix crystallinity (line is drawn to highlight the trend). Two blends display a comparable crystallinity (31.7 and 31.1%), but distinctly reveal a different T_{bd} which most likely can be attributed to their different interparticle distances. A divergence is seen for the blends prepared at 180 °C, displaying a different T_{bd} although their morphological characteristics are similar. The correlation between the T_{bd} and the ID thus depends on the crystalline characteristics of the matrix, if the morphological characteristics are similar.

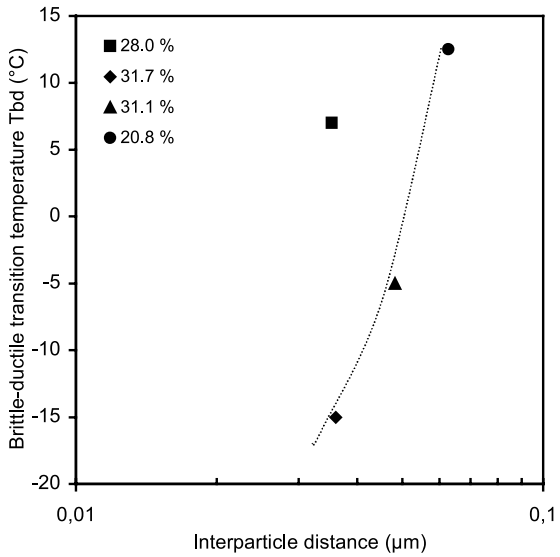

Fig. 19. Brittle–ductile transition temperature as a function of the interparticle distance of the PET/(EPR/E-GMA8) 70/(22.5/7.5) blends prepared at different conditions.

From literature it is known that the matrix crystallinity can strongly affect the yield stress, which increases with increasing crystallinity, especially above the matrix T_g [5,19,22]. Below T_g, this influence is limited, implying a rather small effect on the impact behaviour [37]. Due to the relatively small crystallinity range studied, it can be assumed that the yield stress of the ternary blend systems remains fairly constant. Semicrystalline polymers are known to have a high craze stress. The craze stress is largely independent of the temperature, but increases with increasing entanglement density [2,3,38]. It is therefore not unlikely that an incomplete crystallisation of PET can provoke a decrease of the craze stress as a result of the decreased number of physical cross-links. The PET spherulites crystallised at 180 °C during 0.5 min do not have a sufficient amount of time to grow out completely. It is believed that this incomplete crystallisation can increase the brittle–ductile transition temperature by decreasing the craze stress.

4. Conclusions

The investigation clearly revealed that both the morphological characteristics as well as the impact behaviour of rubber toughened PET are highly influenced by the intrinsic matrix properties. The average particle diameter is found to decrease with an increase of the matrix molar mass. This effect is less pronounced at higher dispersed phase concentrations where the particle size tends to level off at a higher matrix molar mass.

To obtain room temperature tough materials, a minimum matrix molar mass is required. It can be concluded that the effect of the matrix molar mass on the impact behaviour of rubber toughened PET primarily originates from its effect on the blend phase morphology, rather than from an inherent effect of matrix molar mass itself. A direct correlation between the impact strength and the interparticle distance could be established. The critical interparticle distance was determined experimentally at 0.1 μm and appeared to be independent of the matrix molar mass and the dispersed phase concentration. Below ID_c, the impact strength is independent of the matrix molar mass and increases linearly with the interparticle distance. The brittle–ductile transition temperature of the ternary blends with a varying matrix molar mass also displays a strong correlation with the interparticle distance. The T_{bd} decreases when the interparticle distance is decreased, independent of the PET molar mass.

The correlation between the brittle–ductile transition temperature and the interparticle distance depends on the crystalline characteristics of the PET matrix material if the morphological characteristics remain similar. The T_{bd} decreases with decreasing interparticle distance, irrespective of the matrix crystallinity. However, incompletely crystallised PET spherulites lead to an increase of the T_{bd} due to a decrease of the craze stress.

Acknowledgements

The authors are indebted to the IWT-Belgium for a grant to one of them (W. Loyens) and to the KULeuven Research Council for financial support of the laboratory (GOA blend project 98/06). Dr. Luc Leemans of DSM Research is thanked for providing the L-MW and H-MW PET samples.

References

[1] Loyens W, Groeninckx G. Polymer 2002;43:5679–91.
[2] Gaymans RJ. In: Paul DR, Bucknall CB, editors. Polymer blends: performance, vol. 2.; 2000. Chapter 25.
[3] Wu S. Polymer 1985;26:1855–63.
[4] Wu S. Polym Engng Sci 1987;27(5):335–43.
[5] Borggreve RJM, Gaymans RJ, Schuijer J, Ingen Housz JF. Polymer 1987;28:1489–96.
[6] Oshinski AJ, Keskkula H, Paul DR. Polymer 1992;33(2):268–83.
[7] Oshinski AJ, Keskkula H, Paul DR. Polymer 1992;33(2):284–93.
[8] Loyens W, Groeninckx G. Submitted for publication.
[9] Groeninckx G, Dompas D. In: Araki T, Tran-Cong Q, Shibayama M, editors. Structure and properties of multiphase polymeric materials. New York: Marcel Dekker; 1998. Chapter 12.
[10] Borggreve RJM, Gaymans RJ. Polymer 1989;30:63–70.
[11] Cecere A, Greco R, Ragosta G, Scarzini G, Taglialatela A. Polymer 1990;31:1239–44.
[12] Oshinski AJ, Keskkula H, Paul DR. Polymer 1996;37(22):4891–907.
[13] Borggreve RJM, Gaymans RJ, Schuijer J. Polymer 1989;30:71–7.
[14] Dijkstra K, Gaymans RJ. Polymer 1994;35(2):332–5.
[15] Van der Wal A, Gaymans RJ. Polymer 1999;40:6045–55.
[16] Oshinski AJ, Keskkula H, Paul DR. Polymer 1996;37(22):4909–18.
[17] Oshinski AJ, Keskkula H, Paul DR. Polymer 1996;37(22):4919–28.
[18] Hale W, Lee J-H, Keskkula H, Paul DR. Polymer 1999;40:3621–9.

[19] Van der Wal A, Mulder JJ, Oderkerk J, Gaymans RJ. Polymer 1998; 39(26):6781–7.
[20] Martuscelli E, Riva F, Sellitti C, Silvestre C. Polymer 1985;26: 270–82.
[21] Dijkstra K, Ter Laak J, Gaymans RJ. Polymer 1998;35(2):315–22.
[22] Ward IM. In: Ward IM, Hadley DW, editors. Mechanical properties of solid polymers. New York: Wiley; 1993.
[23] Loyens W, Groeninckx G. Macromol Chem Phys 2002;203:1702–14.
[24] Sundararaj U, Macosko CW. Macromolecules 1995;28:2647–57.
[25] Fortelný I, Cerná Z, Binko J, Kovář J. J Appl Polym Sci 1993;48: 1731–7.
[26] Willis JM, Caldas V, Favis BD. J Mater Sci 1991;26:4742–50.
[27] Dedecker K, Groeninckx G. Polymer 1998;39(21):4985–92.
[28] Kudva RA, Keskkula H, Paul DR. Polymer 1998;39(12):2447–60.
[29] Martin P, Devaux J, Legras R, Van Gurp M, Van Duin M. Polymer 2001;42:2463–78.
[30] Van Antwerpen F, Van Krevelen DW. J Polym Sci: Polym Phys, Ed 1972;10:2423–35.
[31] Vu-Khanh T. Polymer 1988;29:1979–84.
[32] Groeninckx G, Reynaers H. J Polym Sci: Polym Phys, Ed 1980;18: 1325–41.
[33] Martuscelli E. Polym Engng Sci 1984;24:563–86.
[34] Groeninckx G, Reynaers H, Berghmans H, Smets G. J Polym Sci: Polym Phys, Ed 1980;18:1311–24.
[35] Bartczak Z, Galeski A, Martuscelli E. Polym Engng Sci 1984;24(15): 1155–65.
[36] Everaert V. PhD Thesis. Catholic University of Leuven, Belgium; 1999.
[37] Gaymans RJ. In: Collyer AA, editor. Rubber toughened polymers. Cambridge: Chapman & Hall; 1994. Chapter 7.
[38] Donald AM. In: Collyer AA, editor. Rubber toughened polymers. Cambridge: Chapman & Hall; 1994. Chapter 1.